Inverse illumination method for characterization of CPC concentrators

A. Parretta[*1,2], A. Antonini[2,4], M. Stefancich[3,4], G. Martinelli[2], M. Armani[5]

[1]ENEA Centro Ricerche "E. Clementel", Via Martiri di Monte Sole 4, 40129 Bologna (BO), Italy.
[2]Physics Department, University of Ferrara, Via Saragat 1, 44100 Ferrara (FE), Italy.
[3]CNR c/o Physics Department, University of Ferrara, Via Saragat 1, 44100 Ferrara (FE), Italy.
[4]CPower SRL Via Saragat 1, 44100 Ferrara (FE), Italy.
[5]Institute for Renewable Energy, EURAC research, Viale Druso 1, 39100 Bolzano (BZ), Italy.
*Phone: +39 (0)51 6098617; Fax: +39 (0)51 6098767; E-mail: antonio.parretta@bologna.enea.it

ABSTRACT

The optical characterization of a CPC concentrator is typically performed by using a solar simulator producing a collimated light beam impinging on the input aperture and characterized by a solar divergence (± 0.27°). The optical efficiency is evaluated by measuring the flux collected at the exit aperture of the concentrator, as function of incidence angle of the beam with respect to the optical axis, from which the acceptance angle can be derived.

In this paper we present an alternative approach, based on the inverse illumination of the concentrator. In accordance with this method, a Lambertian light source replaces the receiver at the exit aperture, and the light emerging backwards at the input aperture is analyzed in terms of radiant intensity as function of the angular orientation. The method has been applied by using a laser to illuminate a Lambertian diffuser and a CCD to record the irradiance map produced on a screen moved in front of the CPC.

Optical simulations show that, when the entire surface of the diffuser is illuminated, the "inverse" method allows to derive, from a single irradiance map, the angle resolved efficiency curve, and the corresponding acceptance angle, at any azimuthal angle. Experimental characterizations performed on CPC-like concentrators confirm these results. It is also shown how the "inverse" method becomes a powerful tool of investigation of the optical properties of the concentrator, when the Lambertian source is spatially modulated inside the exit aperture area.

Keywords (OCIS): Solar energy (350.6050); Optical design of instruments (120.4570); Optical inspection (120.4630); CCD, charge-coupled device (040.1520); Digital image processing (100.2000); Integrating spheres (120.3150).

1. INTRODUCTION

PV concentration systems using nonimaging primary optical elements are valid alternatives to conventional imaging systems using parabolic mirrors or Fresnel lenses[1-3]. Concentrator units of the 3D-CPC family (Ref. [4] Chapt. 4), when suitably modified to shorten their length and model their input aperture in order to have an efficient packing in a module, show several potential advantages: low optical loss, high concentration ratio, low sensitivity to sun tracking errors.

The optical characterization of a CPC concentrator can be performed following a "direct method", that is by sending a collimated beam of solar divergence and known flux to CPC input aperture and measuring the collected flux at the output aperture[5]. The typical experimental setup is that schematically reported in Fig. 1a. The light source (ls) illuminates the integrating sphere (is1) which produces a diffuse light with constant radiance at exit aperture (w). To obtain a light source with the spectrum of the sun, an arc-Xe lamp light source must be used. In addition, a spectrally resolved analysis is also possible by adding the filter (ft). Light from (ls) is preferably modulated at an arbitrary frequency by the chopper (ch), which assures a high sensitivity measurement, decoupled from ambient light.

The parabolic mirror (pm1), oriented off-axis with respect to (w) and at a distance equal to the focal length *f*, collects part of light emerging from the sphere and produces a parallel beam. The maximum angular divergence of the beam is

Optical Modeling and Measurements for Solar Energy Systems, edited by Daryl R. Myers,
Proc. of SPIE Vol. 6652, 665205, (2007) · 0277-786X/07/$18 · doi: 10.1117/12.733605

controlled by the diameter D_w of (w), and the solar divergence (~0.27°) is achieved by operating with a ratio f / D_w ~100. The parallel beam is spatially filtered and directed to the solar concentrator (lc). The light at exit aperture of (lc) is collected by a second integrating sphere (is2) and the flux measured, through photodetector (pd), by the lock-in (li), tuned at the chopper frequency. By orienting the concentrator (lc) at different angles δ with respect to the beam axis, the optical efficiency curve can be drawn. Fig. 1b shows, as an example, the optical efficiency curves obtained simulating an ideal 3D-CPC with δ_{acc} = 5° acceptance angle (Ref. [4] Chapt. 4), 1-cm exit aperture diameter and two wall reflectivities R_w: 0.95 and 1.0. The other dimensional parameters of the CPC are: 11.5-cm input aperture diameter, 71.3-cm length. The efficiency curves are characterized by a quite flat response at low angles and a sharp drop at 50% in correspondence of the acceptance angle, as usual for any ideal CPC concentrator (Ref. [4] Chapt. 4). The acceptance angle can be defined for efficiency drops different to 50%. For photovoltaic applications, for example, it is common to refer to a 10% drop (90% efficiency)[6].

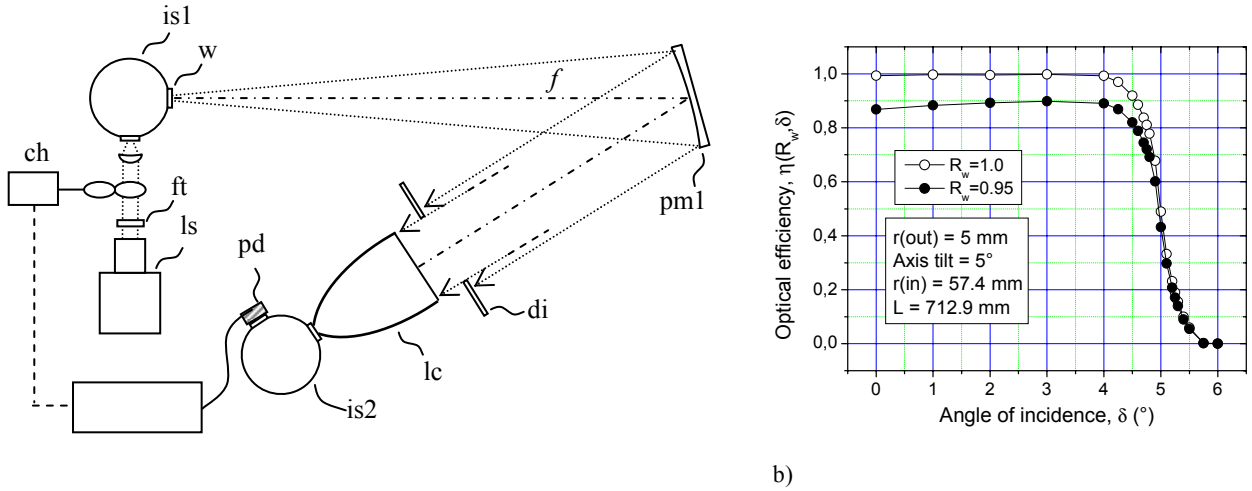

a) b)

Figure 1. a) Schematic of the experimental setup used with the "direct method" for measuring the light collected by a solar concentrator (cpc) at different incidence angles. b) Absolute optical efficiency, or transmittance, curve obtained raytracing an ideal (not truncated) 3D-CPC concentrator with 5° acceptance angle, at two wall reflectivities (1.0 and 0.95).

The simulations were carried out by using the TracePro® software for opto-mechanical modeling[7]. The efficiency curves of Fig. 1b are drawn after a long series of simulations (21 in the examples), or measurements if they are obtained experimentally following the setup of Fig. 1a. In this paper we introduce an alternative way to measure the optical efficiency of the CPC, based on an "inverse" illumination procedure, whereby the CPC exit aperture surface is used as a diffused light source, and the radiant flux of the backward beam, exiting from the CPC at the input aperture, is measured for different directions in space. We will show how this "inverse method" of illumination is particularly attractive for its simplicity, requiring a spatially limited light source (i.e. a laser) and just one simulation or radiation measurement to derive the optical efficiency curve. We will also show how to transform it in a powerful tool for the optical investigation of CPC nonimaging concentrators when the criterion of local illumination of the diffuser is adopted.

2. THE BASIC INVERSE ILLUMINATION METHOD

Fig. 2a shows the schematic principle of the "inverse method". It will be henceforth referred to as ILLUME (Inverse ILLUMination MEthod). The output aperture (oa) of the CPC is closed with a high reflectivity Lambertian diffuser (ld), also called "the target". A collimated light beam (ib), aligned with the optical axis z, is then provided in order to illuminate the entire target area facing the CPC. The incident light is back diffused off the target towards all directions inside the CPC and reflected outside from the input aperture (ia). The output beam (ob) is then projected on a plane, white screen (sc) for visual observation and recording by a digital camera or a CCD, and its intensity distribution studied by changing the screen/CPC distance d. Fig. 2b shows how it appears the illuminated diffuser seen from the input aperture of the CPC. In an alternative scheme, the input beam can be applied from the backside of the concentrator and the high reflectivity diffuser (ld) is replaced by a semitransparent diffuser with Lambertian transmission properties.

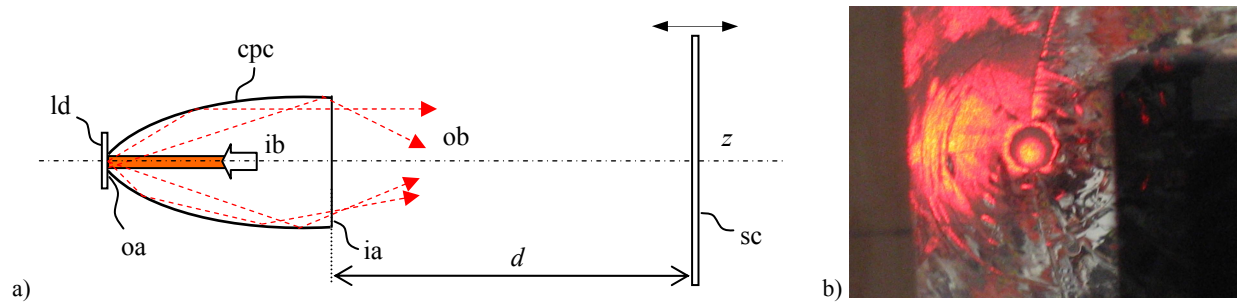

Figure 2. a) Schematic principle of the inverse illumination method (ILLUME). b) Photo of the internal wall of a CPC showing the illuminated diffuser.

As light rays are emitted by diffuser (ld) towards the front side of the CPC from all possible directions, we deduce that the bundle of rays forming the output beam (ob) must correspond to the family of all possible rays which, from the opposite direction, should be able to reach the receiver and then to be collected by the CPC under direct illumination. The inverse illumination method, therefore, provides a bundle of rays (ob) containing all the information related to the collection capabilities of the CPC and, in particular, the information of the CPC acceptance angle. To extract the radiant intensity, $I(\delta)$ in W/sr, produced by the illuminated CPC towards direction δ in the CPC front space, the screen (sc) must be placed far from the CPC, $d >> a$, where a is the radius of the CPC input aperture (ia).

If $E(d, x)$ is the irradiance in W/cm^2 produced on the screen surface at distance x from the z axis, then the radiant intensity for an ideal (not truncated) CPC, with cylindrical symmetry, can be expressed as:

$$I(\delta) = I(d,x) = E(d,x)\cdot\frac{r^2}{\cos\delta} = E(d,x)\cdot\frac{d^2}{\cos^3\delta} = E(d,x)\cdot\frac{d^2}{\cos^3\left[tg^{-1}\left(\frac{x}{d}\right)\right]} \qquad (2)$$

The profile of $E(d, x)$ on the screen, normalized to $E(d,0) = I(0)/d^2$, gives the relative radiant intensity $I_{rel}(\delta)$:

$$I_{rel}(\delta) = \frac{I(\delta)}{I(0)} = \frac{I(d,x)}{I(0)} = \frac{E(d,x)}{E(d,0)}\cdot\frac{1}{\cos^3\left[tg^{-1}\left(\frac{x}{d}\right)\right]} = E_{rel}(d,x)\cdot\frac{1}{\cos^3\left[tg^{-1}\left(\frac{x}{d}\right)\right]} \qquad (3)$$

From what discussed before, it should be clear that the relative radiant intensity $I_{rel}(\delta)$ equals the relative optical efficiency $\eta_{rel}(\delta)$ of the CPC concentrator. In fact, inverting the direction of rays, $I_{rel}(\delta)$ corresponds to the relative (to $\delta = 0°$) flux collected at the CPC exit aperture from a plane wave incident on the CPC input aperture at δ angle. The simplest way to apply ILLUME is to simulate or to measure the "relative" irradiation profile on the screen (sc) and then to derive the "relative" optical efficiency curve and the acceptance angle by applying Eq. (3). In principle we could derive also the "absolute" efficiency curve $\eta(\delta)$ from the ILLUME method, but this implies the knowledge of $\eta(0)$. This is simple to do by simulation, less simple by experimental measurements, because it is required the measurement of $\eta(0)$ by the apparatus of Figs. 1a, which we have tried to avoid.

To verify the arguments so far introduced, we have modeled the ideal CPC with unitary reflectivity introduced in Section 1, operating in the ILLUME mode as schematically described in Fig. 2a. Placing the screen (sc) very far from the CPC, we have obtained a light image with an irradiance profile characterized by a flat top intensity and sharp edges (see Figs. 3a, b). From the irradiance profile, applying Eq. (3), we have derived the relative optical efficiency $\eta_{rel}(\delta)$ vs. incidence angle (see Fig. 3c), measuring an acceptance angle of 5.0°±0.1°, the same obtained by the efficiency curve of Fig. 1b at R_w=1.0. The simulation demonstrates that the ILLUME method gives, in a different way, exactly the same result obtained with the direct illumination method. This relevant result demonstrates the possibility to characterize a nonimaging concentrator by using a simple simulation scheme and only one simulation run. The ILLUME method can be applied also to imaging concentrators (parabolic mirrors, Fresnel lenses) and then it can be considered as a universal method of characterization of optical systems.

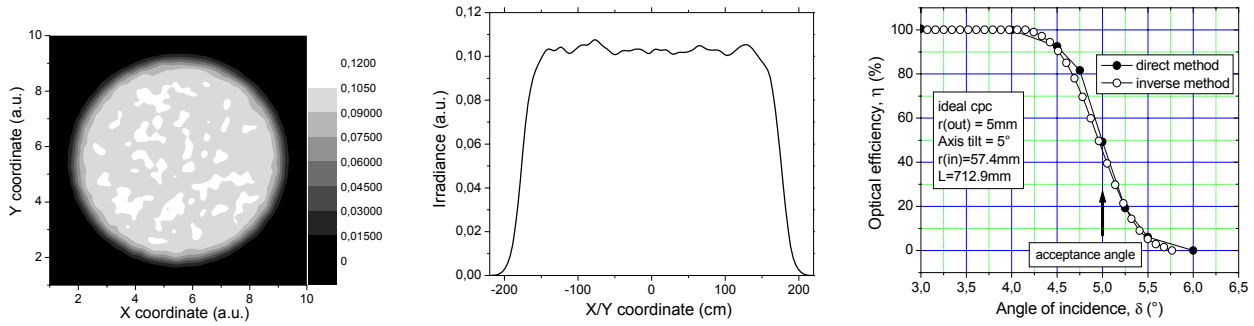

a) b) c)

Figure 3. a) Simulated irradiance map obtained on a 440-cm diameter circular screen distant 2000 cm from the CPC. b) Average x/y profile of the irradiance map. c) Optical efficiency vs. incidence angle curves of an ideal CPC, calculated by following both the direct and the inverse illumination method.

In practice, the ILLUME method is experimentally applied by providing a laser (la) as the collimated light source to illuminate the target (ld) (see Fig. 4). To have the entire target area illuminated as shown in Fig. 2b, the laser beam is spatially modulated by the beam expander (be) and the diaphragm (di). The screen (sc) is then moved in front of the CPC while a CCD monitors and records the light image produced on the screen surface. The irradiance map must be corrected to remove perspective effects introduced by the tilted orientation of the CCD respect to the optical axis *z*. At this purpose, specific codes elaborated by us for the characterization of concentrated solar light beams can be used[8]. In an alternative experimental setup the light source is a lamp (lp) placed behind the CPC and illuminating a semitransparent diffuser; the screen is free to be moved in front of the CPC and the CCD camera can be aligned with the optical axis, avoiding image distortion. This configuration is particularly interesting because it does not require a collimated and a well spatially defined beam (ib) at input. It is sufficient to illuminate the diffuser (ld) with a beam of uniform flux.

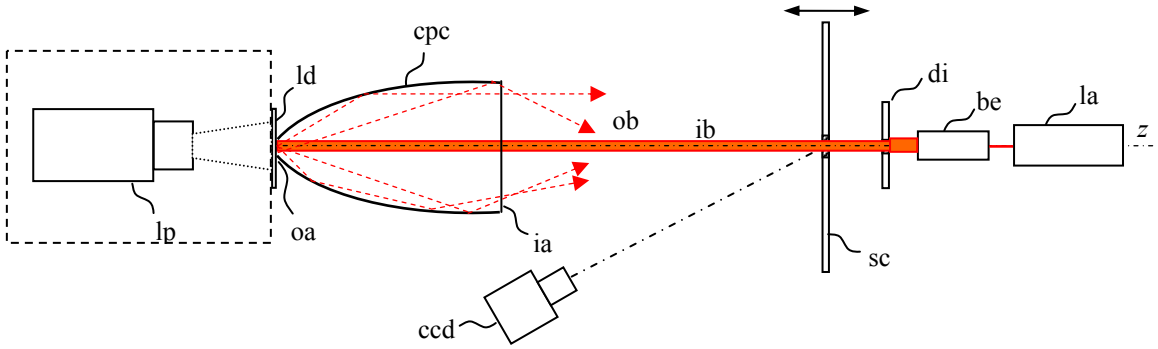

Figure 4. Experimental setup relative to the inverse illumination method (ILLUME). The lamp (lp) in the box can be used in place of the laser (la) if a back illumination is preferred. In this case the CCD camera can be aligned with the *z* optical axis on the right of the screen

3. APPICATIONS OF THE ILLUME METHOD

Optical simulations and experimental characterizations have been performed on some CPC-like concentrators, as simply truncated CPCs and innovative optical units used in concentrator photovoltaic modules[9]. The results confirm the validity of the proposed inverse method.

3.1 Truncated and Squared CPC (TS-CPC)

Fig. 5a shows the CAD of a truncated and a squared CPC (TS-CPC). The original CPC was truncated to reduce its length and its input aperture was squared to give it an external shape suitable to have a high packing efficiency when fabricating an assembly of this units (CPV module). The TS-CPC has a squared input aperture of 10-cm side, a

circular output aperture of 1-cm diameter and a 35-cm length. The prototype was realized by hollowing out a medium density polyurethane prism[10] and coating the internal walls by the VM2002 Radiant Mirror Film of 3M[11] (see the photos of Figs. 2b and 5b). The squaring process produces four planar surfaces which meet at the vertices of the squared aperture. As we shall see, these four surfaces will strongly affect the optical properties of the concentrator. An example of raytracing by ILLUME of the TS-CPC is reported in Fig. 6. The irradiance map, produced on a squared screen (sc) of 500-cm side placed at 3000-cm distance, and the corresponding average profile measured at the centre of the screen along x and y directions, is shown in Fig. 6a and 6b, respectively. The simulated relative efficiency $\eta_{rel}(\delta)$ of the TS-CPC is finally obtained from the irradiance profile by applying Eq. (3) (see Fig. 6c, white circles). The efficiency curve is flat up to ~1.2°, decreases rapidly up to a ~50% value, then decreases slowly. Fig. 6c compares the ILLUME $\eta_{rel}(\delta)$ curve with that obtained by simulating the direct method (dark circles): the agreement is excellent. In practice the two curves should overlap perfectly. The small differences are only the effect of the limited number of rays used in the raytracing process. We find for the inverse method 1.4° and 2.1° as acceptance angles at 90% and 50% efficiency, respectively; the correspondent angles for the direct method are 1.5° and 2.3° (see Table 1).

Fig. 6c also shows the experimental efficiency curve obtained by characterizing the real prototype of TS-CPC with a laser beam at 633 nm wavelength (this method is described in detail in Ref. [5]). The average reflectivity of the prototype internal wall was $R_w = 0.95 \pm 0.01$ at 633 nm[5]. Differences between simulated and experimental curves of Fig. 6c involve several factors: imperfections of TS-CPC wall shape; imperfections of 3M coating surface and loss of light by scattering; wall reflectivity of prototype not perfectly independent of incidence angle; photodetector response not perfectly independent of divergence (zenithal angle) of collected rays; laser characterization realized only on a matrix of points of input aperture (input aperture area not fully illuminated). Despite all these differences between ideal and real conditions, the experimental laser $\eta_{rel}(\delta)$ curve follows quite well that modeled and gives as acceptance angles: 1.1° at 90% efficiency and 2.8° at 50% efficiency (see Table 1).

The ILLUME method becomes a powerful tool of investigation of the optical properties of the concentrator if the diffuser is locally illuminated. In this way in fact we are able to derive the relative efficiency curve $\eta_{rel}(\delta)$ specific of the illuminated area and to establish the range of incidence angles at which that region collects light (is illuminated) by a plane wave at input with less or more efficiency. An example of this procedure is given here simulating the inverse illumination of the centre of the diffuser of TS-CPC by a collimated beam with variable cross section. The irradiance profiles, $E(d, x)$ and $E(d, y)$, recorded on a squared screen of 2000-cm side placed far from the TS-CPC (3000 cm), have been averaged and reported in Fig. 7 for different values of the beam cross section radius. The x and y directions correspond to the TS-CPC input aperture edges (see Fig. 5). The profiles of Fig. 7 are shown at increasing beam cross section radius. The last radius (5 mm) is that required to illuminate the entire diffuser surface. In this case we obtain the same irradiance profile from which the simulated relative efficiency $\eta_{rel}(\delta)$ shown in Fig. 6c (white circles) was derived. The angular interval spanned by the profiles is ±18.4°. It is interesting to note that reducing the beam cross section the efficiency curve reduces in width and increases in height (about twice); as a consequence, also the acceptance angle is reduced. This means that concentrating the inverse beam at exit aperture towards the centre of the diffuser (of the CPC receiver) produces a direct beam at input aperture more aligned with the z optical axis.

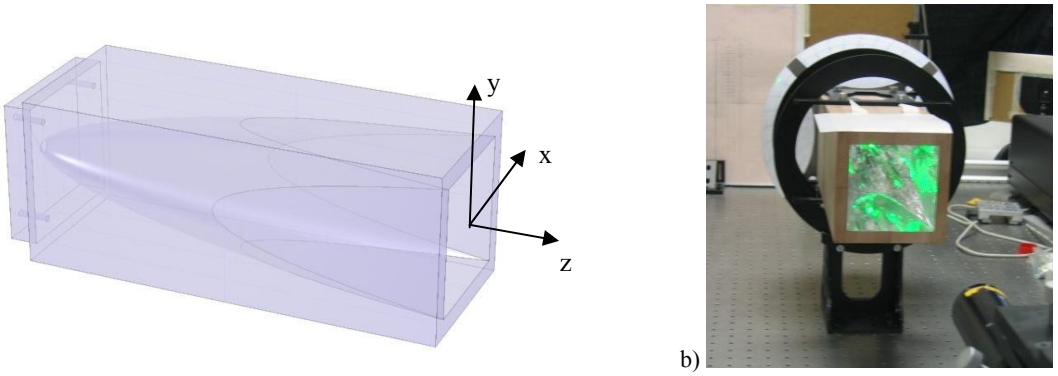

Figure 5. a) Perspective view of the truncated and squared CPC (TS-CPC) model used for simulation experiments with the ILLUME method. b) Prototype of TS-CPC during the laser characterization in laboratory.

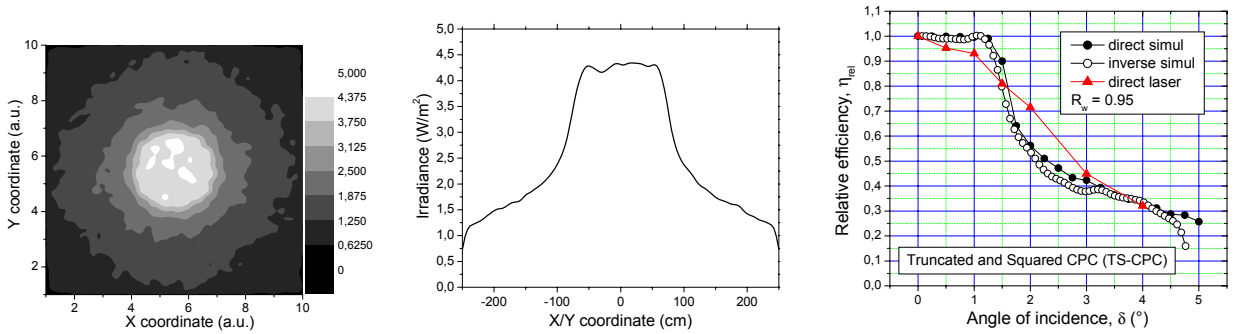

a) b) c)

Figure 6. a) Irradiance map of the TS-CPC concentrator, obtained by simulating the inverse method with a beam (ib) of 5-mm cross section radius. b) Average x/y profile at the centre of the screen. c) Relative optical efficiency, $\eta_{rel}(\delta)$, of TS-CPC obtained by the direct method (dark circles) and the inverse method (white circles). It is also reported, for comparison, the experimental efficiency curve obtained by characterizing the TS-CPC with a laser beam[9] (triangles).

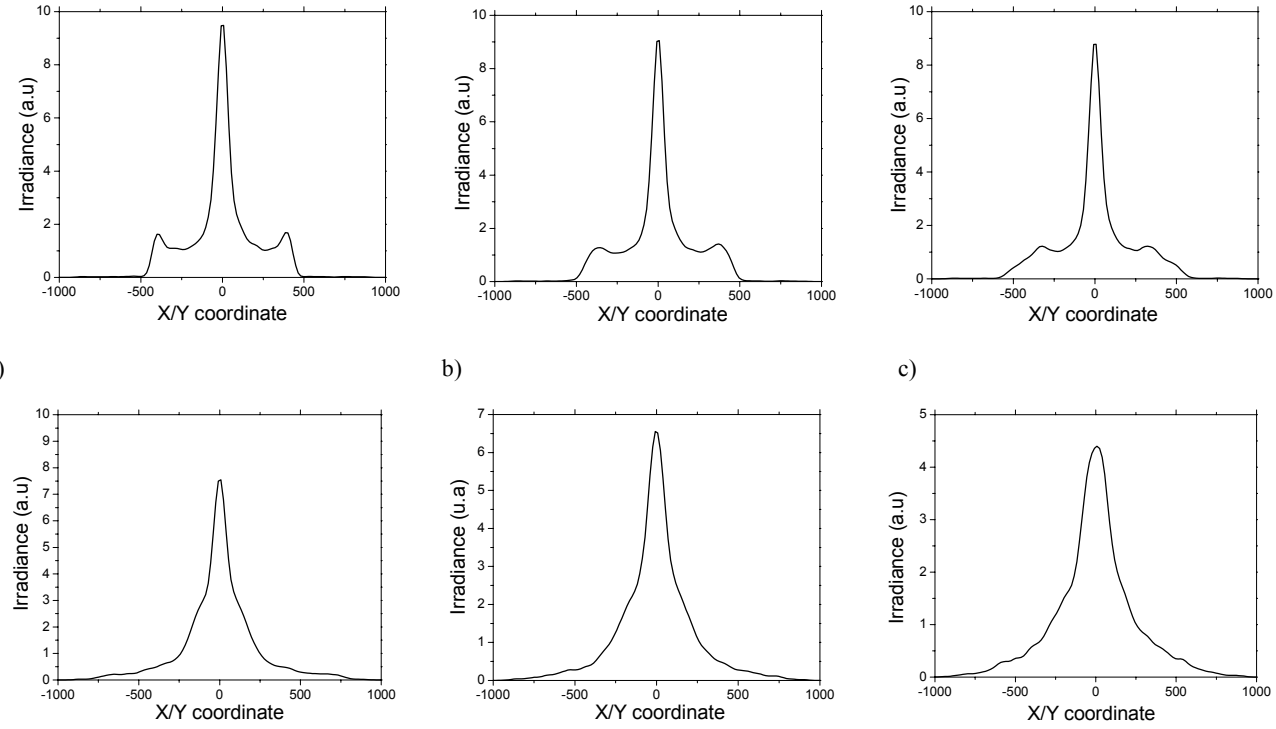

a) b) c)

d) e) f)

Figure 7. Irradiance profiles obtained by simulating (20k rays) the inverse method for the TS-CPC concentrator. The profiles were averaged along *x* and *y* axis directions, parallel to input aperture edges (see Fig. 5a), for different values of the input beam radius. a) R = 0.05 mm (scale 10 W/m^2); b) R = 0.5 mm (scale 10 W/m^2); c) R = 1.0 mm (scale 10 W/m^2); d) R = 2.5 mm (scale 10 W/m^2); e) R = 3.5 mm (scale 7 W/m^2); f) R = 5.0 mm (scale 5 W/m^2).

This is well known in the science of nonimaging optics, that is a beam well collimated with the optical axis of the CPC (δ= 0°) produces an intense irradiation in the very center of the receiver. This is demonstrated here by the simulation of Fig. 8, where the irradiance profile produced on an absorbing receiver of TS-CPC by a plane wave traveling along *z* direction (δ= 0°) is shown. The thinning of the central profile in Fig. 7 goes with the appearing of two satellite bands at ±7.2°. At this angle the square aperture begins the shadowing of the circular receiver respect to an incoming direct beam.

To study the optical efficiency of regions of diffuser (receiver) at different distance from the centre, we have used collimated beams with constant cross section area (π mm^2) but the shape of annulus, with R_{int} and R_{ext} internal and external radius, respectively. The average irradiance profiles are reported in Fig. 9 at increasing values of internal radius R_{int}. If we compare these simulations with those of Fig. 7, we find an enlargement of the profile at increasing R_{int} as well as we found before an enlargement of the profile at increasing R. The shape of the profile in Fig. 9 changes however quite noticeably at high values of R_{int}, when the illuminated region is more peripherical.

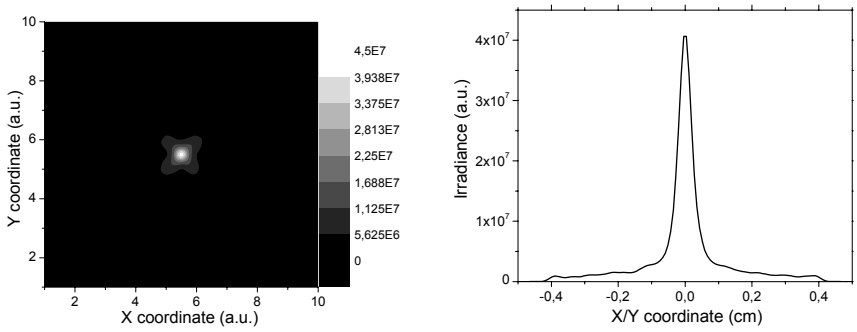

a) b)

Figure 8. a) Simulated irradiance map obtained on the 1-cm diameter receiver of TS-CPC, illuminated by a plane wave aligned with the optical axis. b) Correspondent average irradiance profile along x and y axes (see Fig. 5a).

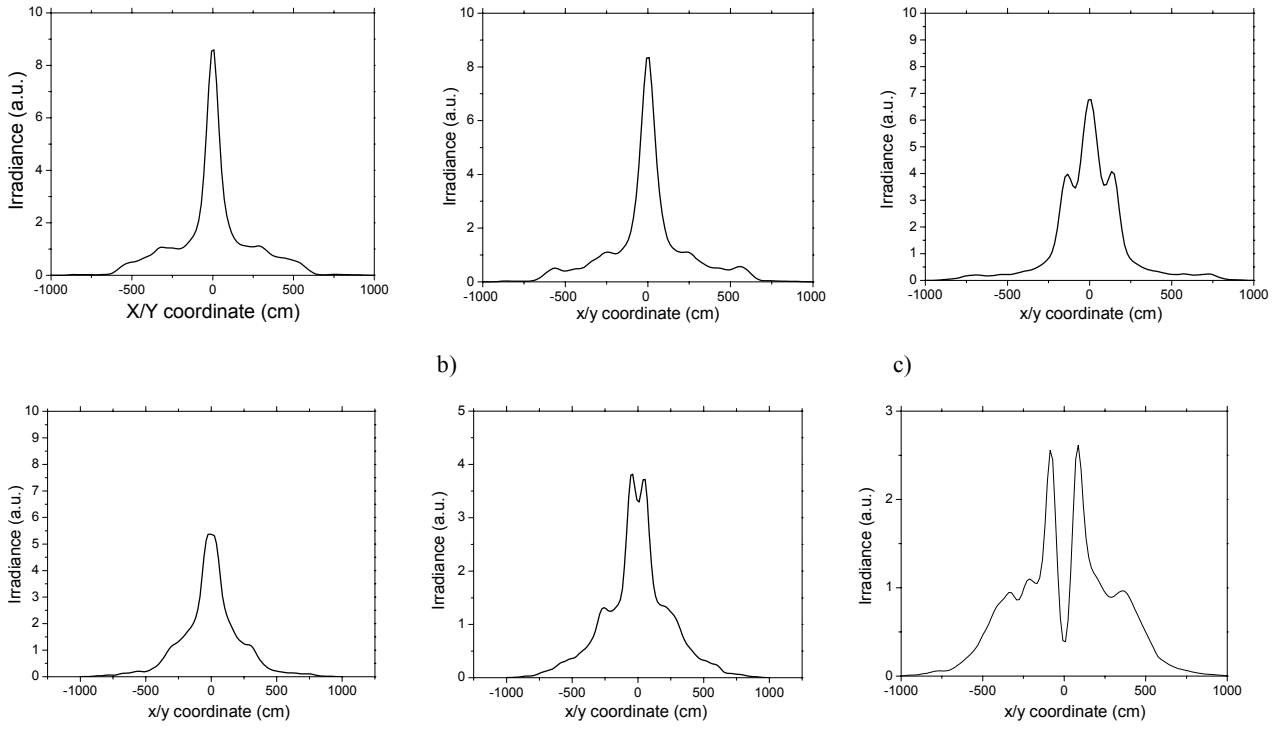

a) b) c)

d) e) f)

Figure 9. Irradiance profiles obtained by simulating (20k rays) the inverse method for the TS-CPC concentrator. The profiles were taken along x and y axis directions, for different values of the internal radius R_{int} of the annulus (the external radius is in parenthesis). a) R_{int} = 0.5 (1.25) mm (scale 10 W/m^2); b) R_{int} = 1.0 (1.414) mm (scale 10 W/m^2); c) R_{int} = 2.0 (2.245) mm (scale 10 W/m^2); d) R_{int} = 3.0 (3.165) mm (scale 10 W/m^2); e) R_{int} = 4.0 (4.123) mm (scale 5 W/m^2); f) R_{int} = 4.9 (5.0) mm (scale 3 W/m^2). The R_{int} = 0.0 (1.0) mm profile has not been shown as it corresponds to that with R = 1.0 mm in Fig. 7.

Here we note the disappearing of the central peak and the formation of two strong satellite peaks symmetric to $\delta = 0°$. This is explained by the same argument used in occasion of the previous simulations, that is that the direct illumination

of the TS-CPC by a z axis aligned beam is not at all able to illuminate the periphery of the receiver, as the profile of Fig. 8 demonstrates. Then, if we illuminate the periphery of the receiver, we cannot extract from the TS-CPC, in the inverse direction, a beam aligned with the z axis. As a consequence, the optical efficiency at near $\delta = 0°$ for the most peripheral region must be very small (Fig. 9e).

Experimental measurements were made following the configuration illustrated in Fig. 4 with the source light (lp) in the box. The semitransparent diffuser (ld) was totally illuminated by the slide projector (lp) (see Fig. 10). The light back diffused by the CPC was thrown on a white screen 345 cm far apart. Fig. 11a shows the light image produced on the screen and recorded by the 8484-05G CCD camera from Hamamatsu Photonics. The image resumes the optical properties of the TS-CPC. We note a squared contour consequence of the squared entrance window (ia). Light protracts over the squared contour as an effect of reflections on the four planar walls. At the centre of the image a strong circular spot is produced. The average intensity profile along x (horizontal) direction crossing the circular spot is obtained from the digitized CCD image. Fig. 11b shows the profile of the relative radiant intensity, $I_{rel}(\delta)$, as obtained by applying the correction $(cos\delta)^3$ term in Eq. (3), which corresponds to the relative optical efficiency $\eta_{rel}(\delta)$ of direct illumination method. From the profile of Fig. 11b we derive an acceptance angle of 0.8° at 90% efficiency and 1.9° at 50% efficiency (see Table 1).

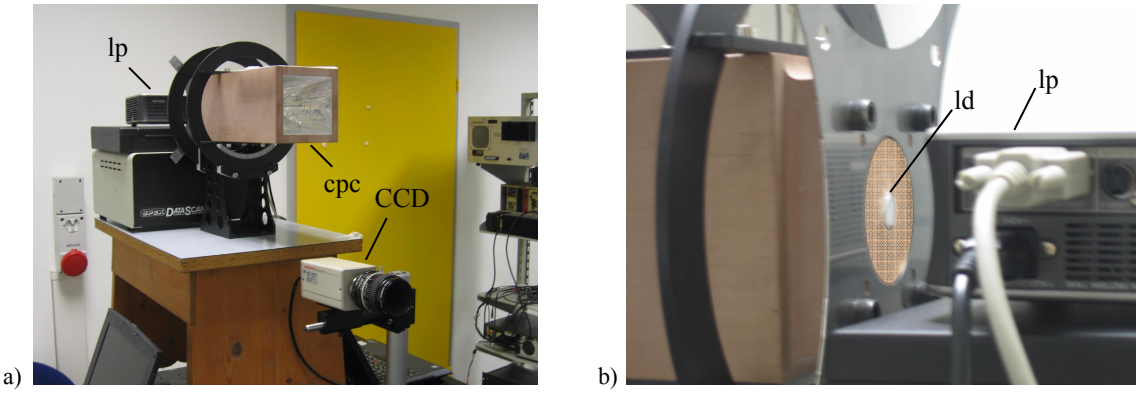

Figure 10. a) Experimental setup of the ILLUME method. The light projector (lp) (see Fig. 4 box) illuminates a semitransparent diffuser (ld) in the back of the TS-CPC. The CCD camera is between the TS-CPC and the screen (sc). b) Particular of the back of TS-CPC.

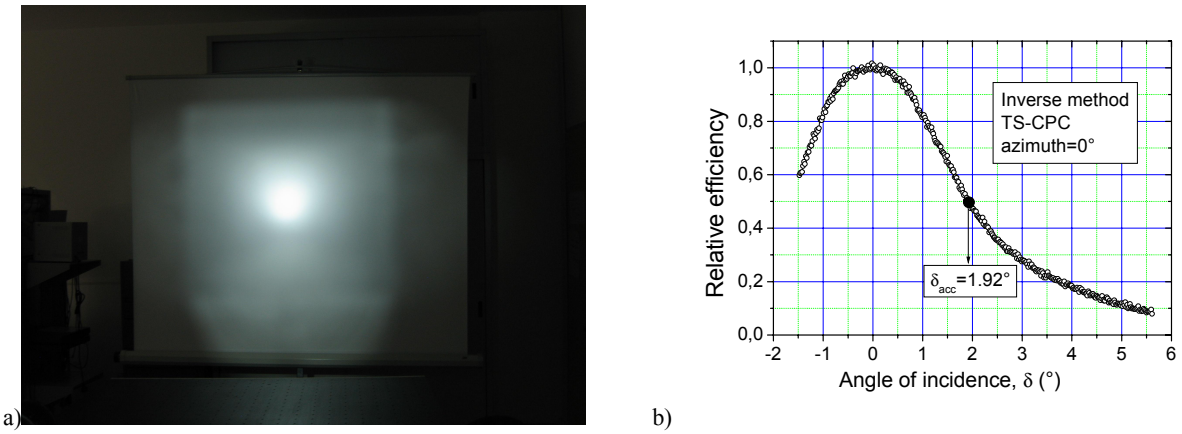

Figure 11. a) CCD image of light diffused on the screen (sc) by the TS-CPC illuminated in the inverse mode (ILLUME). b) Relative radiant intensity profile $I_{rel}(\delta)$, calculated applying Eq. (3) to the relative irradiance $E_{rel}(d, x)$ measured on the screen surface. The radiant intensity profile corresponds to the relative efficiency $\eta_{rel}(\delta)$ of the CPC concentrator.

3.2 Half Truncated CPC (HT-CPC)

To better understand the influence that modifications of the ideal CPC have on the irradiance profile of inverse illumination, we have modeled a truncated but not squared CPC, with a circular instead of a squared input aperture. The ideal CPC described in the Introduction was halved, obtaining a half-truncated CPC (HT-CPC). The dimensional parameters of the HT-CPC are: 1-cm diameter exit aperture, 10.4-cm diameter input aperture (~85 cm^2 input area), 35.8-cm length. From them we derive a geometric concentration ratio C_{geo}=108x (Ref. [4] Chapt. 1), and from the equation $C = 1/\sin^2 \delta_{acc}$ (Ref. [4] Chapt. 2) we expect an acceptance angle $\delta_{acc} \sim 5°$. This value will be confirmed by simulations with both direct and inverse methods. HT-CPC is similar to TS-CPC in the dimensional parameters, but the different shape of entrance aperture, in particular the presence in TS-CPC of the four planar surfaces (see Fig. 5), renders their response to inverse method very different. Fig. 12a shows the schematic of half-truncated CPC (HT-CPC).

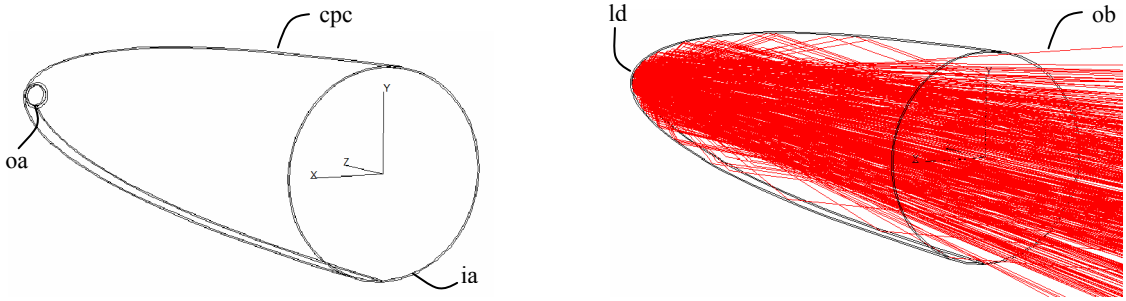

Figure 12. a) Schematic of the half-truncated CPC (HT-CPC) used for experiments with the ILLUME method. b) Example of raytracing by TracePro[7] of the HT-CPC, illuminated in inverse way by a beam of 10 mm diameter.

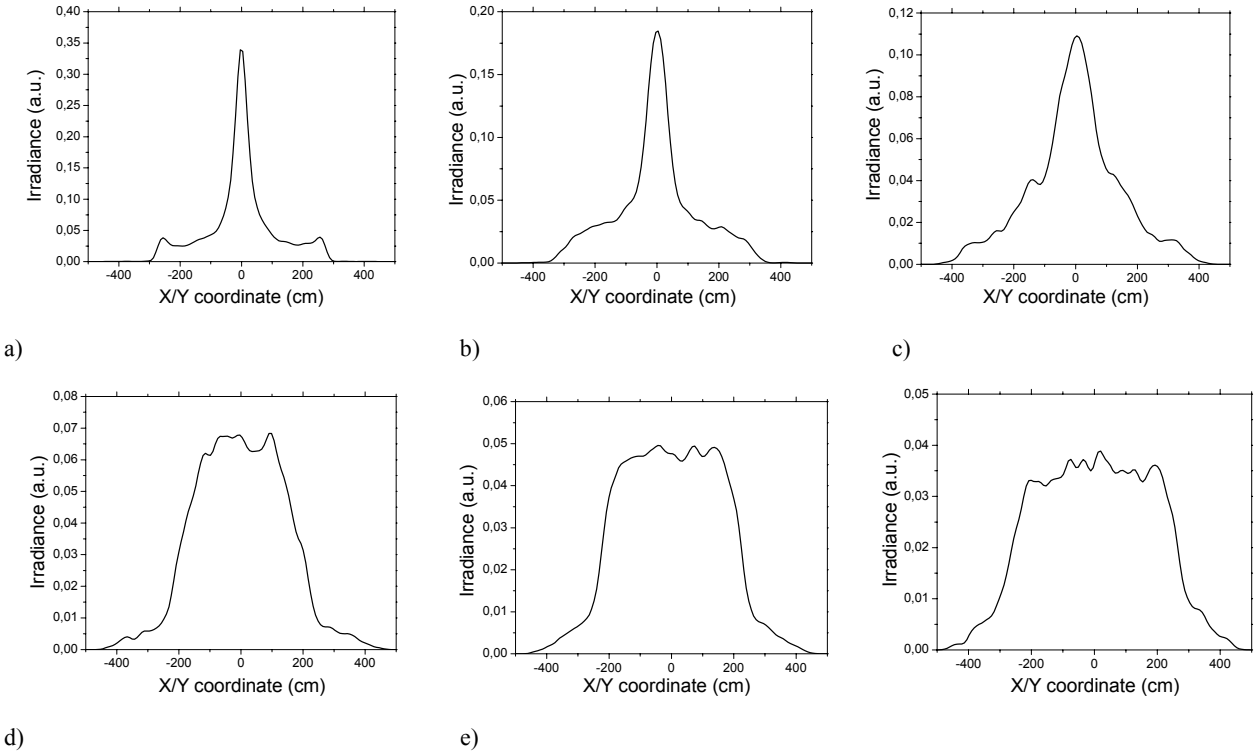

Figure 13. Irradiance profiles obtained by simulating the inverse method for the HT-CPC. The profiles were taken at different cross sections of the input beam (ib), centered on the diffuser. a) R = 0.05 mm (scale 0.4 W/m^2); b) R = 0.5 mm (scale 0.2 W/m^2); c) R = 1.0 mm (scale 0.12 W/m^2); d) R = 2.5 mm (scale 0.08 W/m^2); e) R = 3.5 mm (scale 0.06 W/m^2) e) R = 5.0 mm (scale 0.05 W/m^2).

Applying a Lambertian diffuser at the output aperture (oa) and illuminating it by a collimated beam (ib) from a laser (la), as illustrated in Fig. 4, we were able to perform optical simulations with the ILLUME method. An example of raytracing by TracePro of the HT-CPC is shown in Fig. 12b.

As for the TS-CPC, we have simulated the inverse illumination of the centre of the diffuser by a beam with variable cross section. The screen (sc) is of 1000-cm diameter at 3000-cm distance from the entrance window (ia). The irradiance profiles, $E(d, x)$ and $E(d, y)$, at the centre of the screen (sc) have been averaged and reported in Fig. 13 for different values of the beam cross section radius R. They too show the existence of satellite peaks similar to those obtained with the TS-CPC (see Fig. 7).

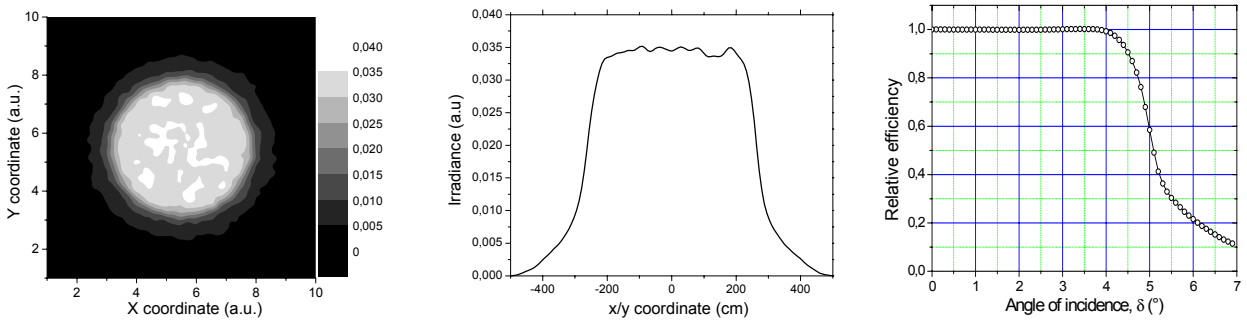

a) b) c)

Figure 14. a) ILLUME irradiance map obtained by raytracing (100k rays) the HT-CPC with a collimated beam of 5.0 mm radius incident on the centre of the diffuser. b) Irradiance profile recorded on the screen (sc). The acceptance angle is 4.5° for 90% efficiency and 5.1° for 50% efficiency (see Table 1). c) Relative efficiency calculated by simulating the direct method of illumination for the HT-CPC. The acceptance angle is 4.5° for 90% efficiency and 5.1° for 50% efficiency (see Table 1).

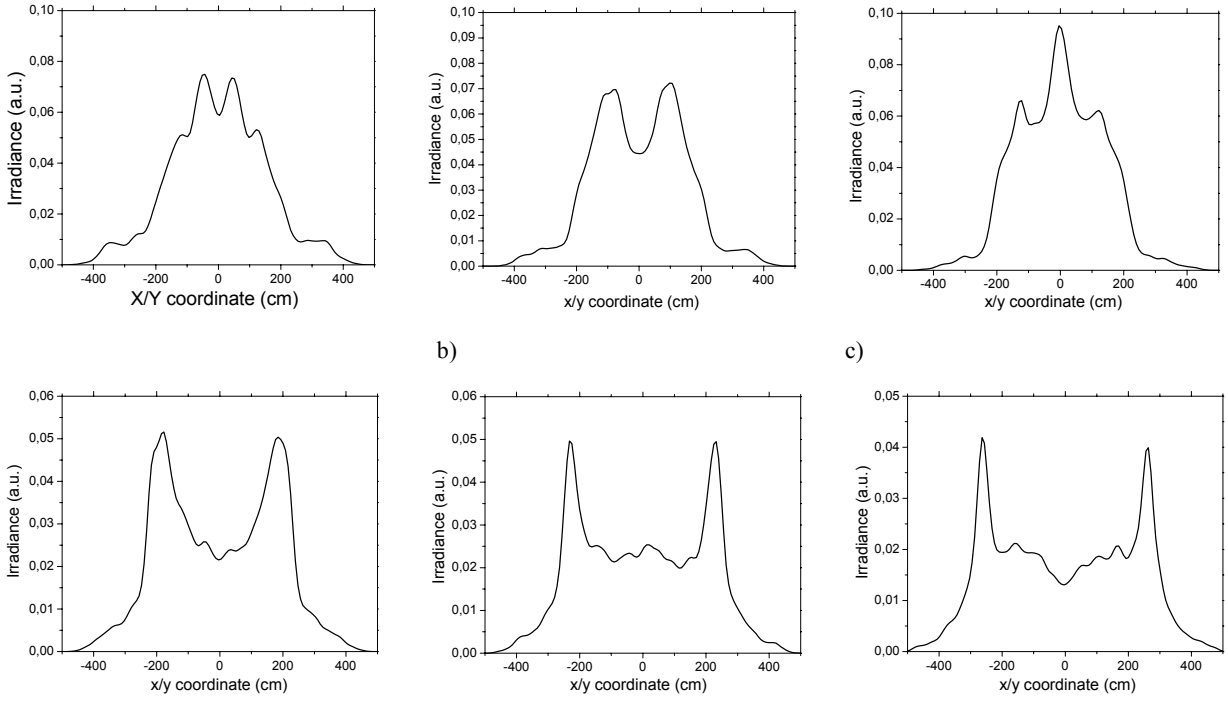

a) b) c)

d) e) f)

Figure 15. Irradiance profiles obtained by simulating (50 krays) the inverse method for the HT-CPC concentrator (50krays). The profiles were taken along x and y axis directions, for different values of the internal diameter D_{int} of the annulus (the external diameter is in parenthesis). a) R_{int} = 0.5 (1.25) mm (scale 0.1 W/m^2); b) R_{int} = 1.0 (1.414) mm (scale 0.1 W/m^2); c) R_{int} = 2.0 (2.245) mm (scale 0.1 W/m^2); d) R_{int} = 3.0 (3.165) mm (scale 0.06 W/m^2); e) R_{int} = 4.0 (4.123) mm (scale 0.06 W/m^2); f) R_{int} = 4.9 (5.0) mm (scale 0.05 W/m^2).

The profiles of Fig. 13 spans an angle of incidence of ±9.5°, and the more pronounced satellite peaks are centered at ±4.7°. Differently from those of TS-CPC, the profiles of HT-CPC change drastically in shape with increasing the beam cross section radius, and the intensity decreases sevenfold. Increasing beam radius, the satellite peaks, well visible in Fig. 13a at R = 0.05 mm, disappear at R~0.25 mm, leaving a broad background; the central peak decreases progressively up to disappearing, and the broad peak transforms in the large and top-flat peak typical of ideal CPCs. This means that, even halved, an ideal CPC maintains quite unchanged its optical behavior. The accurate simulation with R = 5 mm (see Fig. 14) gives the HT-CPC relative optical efficiency with an acceptance angle of 4.5° at 90% efficiency and of 5.1° at 90% efficiency (see Table 1). The value obtained at 50% efficiency confirms the theoretical value obtained applying the formula for the concentration ratio: $C = 1/(\sin \delta_{acc})^2$. The irradiance profiles relative to the inverse illumination of HT-CPC with beams of constant cross section area (π mm^2) and shape of annulus are reported in Fig. 15. Also these profiles differ strongly from the correspondent ones of TS-CPC concentrator. This demonstrates that, even though similar dimensionally, the TS-CPC and HT-CPC concentrators show a strong difference in optical behavior due to the different shape of the input aperture and of the internal wall.

Method		Ideal 3D-CPC		TS-CPC		HT-CPC	
		90% Eff	50% Eff	90% Eff	50% Eff	90% Eff	50% Eff
Direct	Simulated	4.5°	5.0°	1.5°	2.3°	4.5°	5.1°
	Experimental			1.1° (laser)	2.8° (laser)		
Inverse	Simulated	4.5°	5.0°	1.4°	2.1°	4.5°	5.1°
	Experimental			0.8°	1.9°		

Table 1. Summary of the values of acceptance angle obtained by simulated and experimental measurements of the direct and inverse method, for the 3D-CPC concentrators tested in this paper. The acceptance angles are referred to both 90% and 50% efficiency values. The data of TS-CPC refer to α = 0° azimuth.

4. CONCLUSIONS

In conclusion, we have introduced a new method of characterization of solar concentrators, called ILLUME, whose experimental setup is very simple to realize, requiring only a laser or a lamp and a digital camera or a CCD. By this method, a single simulation or a single experimental measurement is sufficient to determine the relative optical efficiency and the acceptance angle of the concentrator. We have tested the ILLUME method on different types of nonimaging concentrators, by simulations with commercial optical codes and by experimental measurements. In all cases, the optical efficiency and the acceptance angle were consistent with those attainable with conventional optical methods of characterization.

ACKNOWLEDGMENTS

We acknowledge the support of P. Colombani and E. Chiodelli (Photo Analytical Srl).

REFERENCES

[1] G. Martinelli, c. Malagù, M. Stefancich, D. Vincenzi, A. Parretta and R. Winston, "Optical beam splitting and CPC for high performances photovoltaic concentrator systems" oral presentation at the "19th Congress of International Commission for Optics, ICO XIX, Optics for the Quality off Life", Firenze, 25-30 August 2002. Technical Digest vol. II, ed. By A. Consortini and G.C. Righini (Washington, USA: SPIE Vol. 4829) 2002, pp. 1023-1024.

[2] A. Parretta, G. Martinelli, M. Stefancich, D. Vincenzi and R. Winston, "Modelling of CPC-based photovoltaic concentrator" oral presentation at the "19th Congress of International Commission for Optics, ICO XIX, Optics for the Quality off Life", Firenze, 25-30 August 2002. Technical Digest vol. II, ed. By A. Consortini and G.C. Righini (Washington, USA: SPIE Vol. 4829) 2002, pp. 1011-1012.

[3] A. Parretta, M. Morvillo, C. Privato, G. Martinelli and R. Winston, "Modelling of 3D-CPCs for concentrating photovoltaic systems" oral presentation at the Conference "PV in Europe, from PV Technology to Energy Solutions", Rome, Italy, 7-11 October 2002. Ed. J.L. Bal, G. Silvestrini, A. Grassi, W. Palz, R. Bigotti, M. Gamberane, P. Helm. WIP-Munich and ETA-Florence, 2002, pp. 547-550.

[4] R. Winston, J.C. Miñano and P. Benítez, "*Nonimaging Optics*" Elsevier Academic Press, Burlington, MA 01803, USA, 2005.

[5] A. Parretta, A. Antonini, M. Stefancich, V. Franceschini, G. Martinelli, M. Armani, "Characterization of CPC solar concentrators by a laser method", oral presentation 6652-06 at this Conference, "Optical Modeling and Measurements for Solar Energy Systems", Session 1, "Solar Energy Systems and Components" .

[6] A.W. Bett, F. Dimroth, S.W. Glunz, A. Mohr, G. Siefer, G. Willeke, "FLATCON™ and FLASHCON™ concepts for high concentration PV", Proc. Of the 19th EPSEC, 7-11 June 2004, Paris. Ed. W. Hoffmann, J.-L. Bal, H. Hossenbrink, W. Palz, P. Helm, WIP-Munich and ETA-Florence, 2004, pp. 2488-2491.

[7] Lambda Research Corporation, 80 Taylor Street, P.O. Box 1400, Littleton, MA 01460, http://www.lambdares.com/.

[8] A. Parretta, C. Privato, G. Nenna, A. Antonini, and M. Stefancich, "Monitoring of concentrated radiation beam for photovoltaic and thermal solar energy conversion applications", Applied Optics **45**, 7885-7897, 2006.

[9] A. Antonini et al., "Modeling of CPCs for concentrator photovoltaic applications", in preparation for Solar Energy.

[10] Paolo Colombani Design, Ferrara, Italy, www.paolocolombani.com.

[11] www.3m.com/radiantlightfilm